November 8, 2001

E94010 Unpolarized ^{3}He Cross Sections v. 1.0

K. Slifer
Temple University,
Philadelphia, PA 19122, USA
E-mail: kslifer@temple.edu

Contents

1 Introduction

We will discuss the unpolarized ^{3}He cross sections of E94010 as well as make an estimate of the systematic errors associated with this measurement. In this note, we summarize how the cross section inputs such as charge, density, etc. are determined and list best values for these quantities. Known problems with the data, as well as difficulties with the detector equipment will also be listed.

2 Cross Sections

The experimental cross section before radiative corrections is given by:

$$\frac{d\sigma}{dE'd\Omega} = \frac{N_f}{N_i \rho t \Delta E' \Delta\Omega} \times \frac{1}{(1-Dt)} \frac{1}{(1-\epsilon_{det})} \frac{1}{(1-\epsilon_{cut})} \tag{1}$$

Where:

1. N_f : Number of scattered electrons detected.
2. N_i : Number of incident electrons. This is determined from the charge. The charge (in μC) is extracted from the DownX10 scaler using the following conversion constants (from A. Saha).

Table 1.

Current(μA)	Conversion Constant
0.0 - 1.0	31322.0
1.0 - 5.0	32838.0
5.0 - 10.0	33245.0
10.0 - 20.0	33393.0
> 20.0	33393.0

3. ρ: density of target (in cm^{-3}), corrected for temperature(from I. Kominis).

Table 2.

Target	Density (Amagat)
Don't Worry	12.249
Blue	10.0
Armageddon	12.324
Be Happy	11.533
Nephali	13.778
Syshiphos	9.942
Jin	10.236
Cuervo	9.309

4. t : length of target (cm)

5. ΔE' : Scattered electron energy spread (MeV). The central momentum settings have been corrected for hysterisis effects using spectrometer constants given by N. Liyanage[5]. For reference we also list the best determination of incident energies for E94010.

Table 3. Incident Energies
1717.9
3381.8
1716.9
4238.6
862.0
2580.5
5058.2

6. $\Delta\Omega$: Angular Acceptance (Sr). Simulated by X. Jiang[4].

7. Dt : Detector Deadtime. Evaluated from the Scalers.

$$DT = 1.0 - Prescale \times \frac{T^*}{T}$$

   where T^* is the number of triggers recorded to tape, and T is the number of triggers recorded by the scalers.

8. ϵ_{det} : Detector Efficiency[6,7,8].

9. ϵ_{cut} : Software Cut Efficiency.[6,7].

The resulting cross sections are shown if Figs. 1 to 7.

3 Cut Variation

To evaluate the performance of the acceptance simulation, we have examined how sensitive the cross section is to variations in the acceptance cut. The table below lists the ten cuts utilized in the study. Here, $\phi(\theta)$ represents the horizontal(vertical) scattering angle evaluated at the target with respect to the central ray of the spectrometer. z represents length along the target with z=0 at the target center. Cut number three is the actual cut used to produce final cross sections. It has been chosen by comparing simulated target variables to actual data. Details of the analysis cut are discussed in [3]. Notice cuts 4 to 7 are asymmetric cuts and that 6 and 7 in particular represent “garbage” cuts.

Table 4. X-Sect. Acceptance Cuts			
CUT	ϕ (mrad)	θ (mrad)	z (mm.)
1	±5	±30	±60
2	±15	±10	±60
3	±15	±30	±60
4	±15	±30	$-60\leq z\leq 00$
5	±15	±30	$00\leq z\leq 60$
6	±15	±30	≥60
7	±15	±30	$\leq$-60
8	±15	±30	±15
9	±15	±30	±30
10	±15	±30	±90

The resulting cross section for each cut is compared to the cross section of cut # 3.

$$\Delta X_i = \frac{A_i - B_i}{A_i} \times 100.00 \tag{2}$$

Here

- A_i is the optimized cross section of cut # 3
- B_i is the alternative cross section, obtained using a different cut.
- i refers to a particular bin in ν.

Then the percent difference is calculated using the following:

$$\sigma^2 = \frac{\sum \Delta X_i^2/\nu_i}{\sum 1/\nu_i} \tag{3}$$

The weighting by $1/\nu$ is performed to account for the fact that the cross sections enter the GDH Sum weighted by $1/\nu$. Also the summation begins at the pion threshold for that energy, shown in the table below.

Table 5.	
$E_0(MeV)$	Pion Threshold in ν (MeV)
862.0	171.2
1716.9	246.0
2580.5	369.3
3381.8	522.9
4238.6	725.4
5058.2	953.0

From the definition given above, we can see that the result is a measure of how the cross section uncertainty affects the integral, and not truly a measure of our cross section systematic, which would be bigger. The result for each energy is shown in the table below.

Table 6. X-Sect. Cut Variation (Percentage)

	862	1717		2591	3382	4239		5058
		1st	2nd			nephali	sysiphos	
1	0.8	1.0	1.3	1.3	1.8	**3.3**	1.9	1.7
2	0.6	0.8	1.2	1.7	2.0	2.2	2.2	**2.4**
3	0.0	0.0	0.0	0.0	0.0	0.0	0.0	0.0
4	3.9	0.7	1.8	2.2	2.8	4.5	6.7	2.7
5	3.7	0.7	1.7	2.1	2.8	4.4	5.8	2.6
6	7.0	5.3	9.3	11.8	14.9	22.1	14.5	13.0
7	4.0	4.3	11.6	13.8	17.0	24.5	16.3	15.3
8	**2.8**	**2.4**	**1.6**	**2.0**	**2.0**	2.0	**2.2**	1.9
9	1.4	0.8	0.8	0.8	0.8	0.8	1.0	1.0
10	0.5	0.4	0.4	0.5	0.5	0.5	0.7	0.7

4 Other Systematics

Below we list the other contributions to the total cross section systematic.

1. Detector Efficiencies
   - Čerenkov: < 1% correction [6]
   - Shower : < 1% correction [7]
   - VDC : 1% correction [8]
   - Scintillator : Very large correction. Error should be of order 1 %. Needs to be verified. Comparison of 862 MeV cross section with and without T2 correction indicates that correction is being done properly. See Fig. 17.
2. Cut Efficiency
   - Čerenkov: < 1% correction [6]
   - Shower : < 1% correction [7]
   - Wire : ?
   - Scintillator: ?
3. Target Reconstruction [9]

- y_{targ} : 1.6 %
- θ, ϕ : 2.0 %

4. Other [1].

    - Deadtime : assuming negligible.
    - Charge : 1.0 %
    - N_2 : 0 %
    - Incident Energy: 0.5 %

Chosing the largest cut variation for each energy and adding the remaining systematics in quadrature we obtain the total systematic errors shown in the table below.

5 Spectrometer Difference

The fact that we employed two completely independent spectrometers during E94010 allows us to also estimate our systematic by comparing the cross section measured by the two arms. We perform a similar study as the previous cut analysis using equations 2 and 3, but here

- A_i is the cross section of cut # 3 for the electron arm
- B_i is the cross section of cut # 3 for the hadron arm.

The resulting weighted average for each energy is shown in the following table along with the total systematic found in the previous section.

Table 7.

E_0	Total Systematic Error	Spectrometer difference
862	4.5 %	10.4 %
1717 (1st per.)	4.3 %	1.2 %
1717 (2nd per.)	3.9 %	5.2 %
2591	4.1 %	3.4 %
3382	4.1 %	3.9 %
4239 (nephali)	4.9 %	— %
4239 (sysiphos)	4.2 %	3.5 %
5058	4.3 %	4.4 %

The hadron arm data is unreliable for 862 MeV (see Section: Known problems) so we should not be surprised that the spectrometers do not agree very well for this energy. And the 1st period for 1717 MeV comprises a small quantity of data at large ν, so the result is not reliable. For the other energies the agreement of the two methods is reasonable. Disregarding the quasielastic contribution and weighting the comparison by $1/\nu$ accounts for the smaller systematic estimate given by comparing spectrometer results.

6 Known Problems

Here we discuss the known problems of the E94010 cross sections. Where applicable, the remedy is described.

1. The missing kinematic from $\nu = 261$ to 380 MeV for $E_0 = 862.0$ MeV. See Fig. 1.

2. Blockage of the Hadron arm acceptance for $E_0 = 862.0$ MeV. This is presumably caused by hanging rtd wires. See Figs. 19 and 20. This casts doubt on the validity of the hadron arm data for this entire energy setting. Attempts at isolating and removing the problem data using cuts were unsuccessful.

3. The 1 MeV energy shift(Fig. 18) in the hadron arm at $E_0 = 862.0$ MeV. During the 862 MeV energy setting, E94010 recorded elastic scattering data for the first few runs using both spectrometers and again at the completion of helium data taking for this energy using only the hadron arm. During the early elastic data, the two arms agree. However the elastic peak in the hadron arm is found to be shifted by one MeV for the later runs.

4. Mismatching of quads and dipole for electron arm lowest three momentum settings of $E_0 = 862.0$ MeV. The Hall A NMR probe was unable to track the dipole field below about 400 MeV during E94010. Instead, the gauss meter was used for the lowest three momentums. Unfortunately, the device was not properly calibrated. As a result the dipole was fixed incorrectly at a different momentum than the quadrupoles for the three final electron arm kinematics. To minimize the effect of the mismatched quads, cut number 1 from Table 1 was used for these three kinematics to select central events. Also the current from the dipole was used to determine the true dipole central momentum(See Figs. 15 and 16). The results are shown in green in Fig. 1.

5. Mismatching of quads and dipole for single hadron arm momentum for $E_0 = 1717$ Me V. This is a problem similar to the previous point. See Fig. 2

6. The rising tail of the cross section for E_0 = 862 MeV and 1717 MeV. See 1 and 2. The rising tails can not be explained in terms of radiative corrections, or nitrogen contamination. These two possibilities were investigated by S. Choi and found to be unsatisfactory. Examination of the asymmetries corresponding to this data show that the tails are unpolarized.

7. Lowering of the scintillator discrimination threshold near end of data taking of E94010. Nilanga wrote a report on this topic.[2]

7 Acknowledgements

Thanks to J.P. for clarifying many issues regarding the cross section systematics.

8 References

1. G. Cates, A. Deur. Private communication. Nov. 2, 2001.
2. N. Liyanage. *HRSH inefficiency corrections for 2.591 and 5.07 GeV running.* (2000). www.jlab.org/∼nilanga/physics/94010/5GeV_scaler.ps
3. K. Slifer. *Dependence of the Cross-Section on Acceptance Cuts for E94010.* E94010 Technical Note **37**. (2001)
4. X. Jiang. *Acceptance Function of Hall-A E94010 Experiment.* E94010 Technical Note. (2000)
5. Implemented by I. Kominis,K. Slifer. Results can be found on JLAB CUE machines at: /home/slifer/src/datafiles/momentum_settings.dat
6. K. Slifer. *Shower Detector Calibration and Cut Optimization for E94010.* E94010 Technical Note **31**. (2000)
7. K. Slifer. *Analysis of the Hall A HRS Čerenkov Detectors for E94010.* E94010 Technical Note **32**. (2000)
8. A. Deur, Vertical Drift Chambers Analysis. E94010 Technical Note **29**. (1999)
9. N. Liyanage. *Study of systematic uncertainties for cross section measured in E94-010.* (2001). www.jlab.org/∼nilanga/physics/94010/cross_section.ps

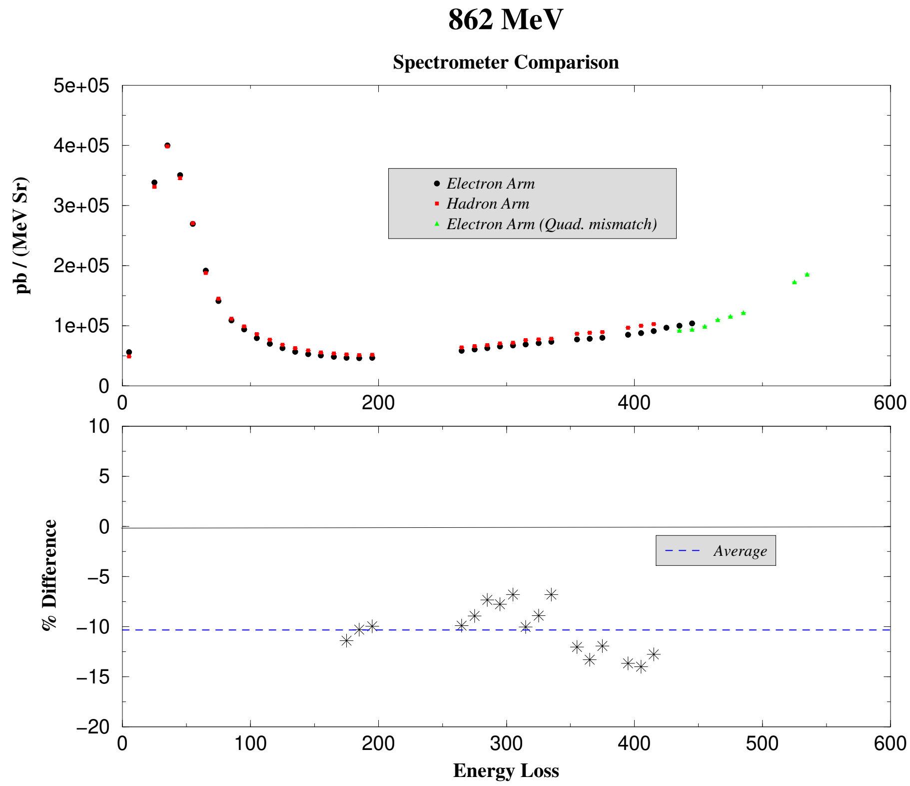

Figure 1: 862 MeV cross section. Top Panel: Black is Electron arm. Red is Hadron arm. Green is Electron arm with correct dipole momentum and selecting only central events. Lower Panel: (E-H)/E X 100. Blue dashed line represents the *unweighted* average.

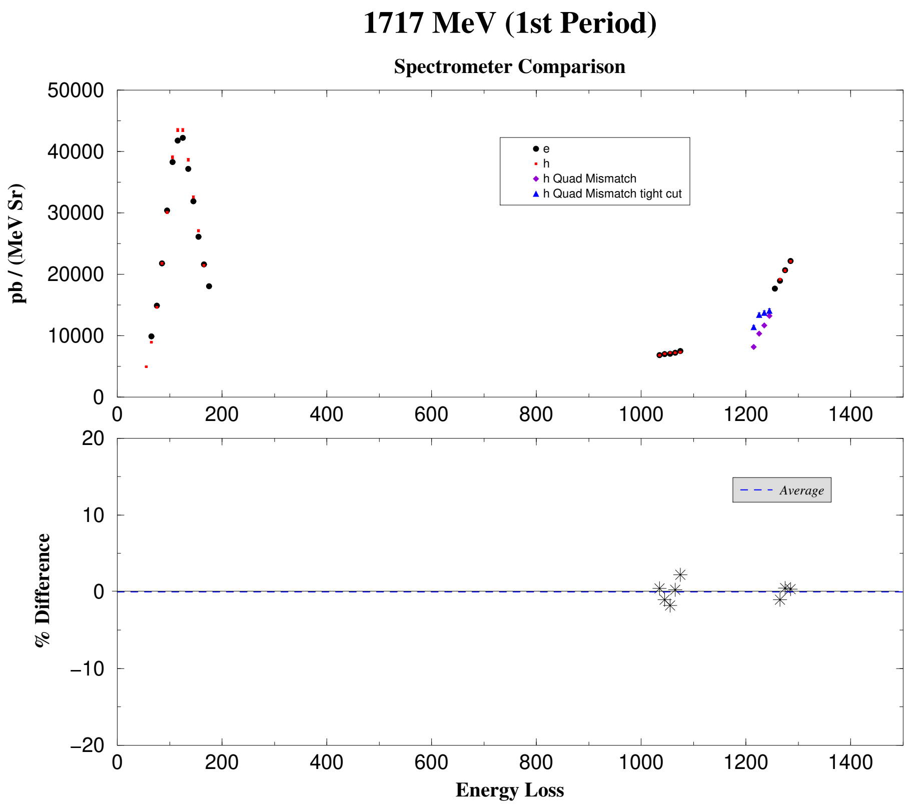

Figure 2: 1717 MeV, 1st period. Top Panel: Black electron arm. Red hadron arm. Purple diamond is hadron data with mismatched quad and dipole. Blue triangle is same data with tight cut to minimize quadropole effect. Lower Panel: (E-H)/E X 100. Blue dashed line represents the *unweighted* average.

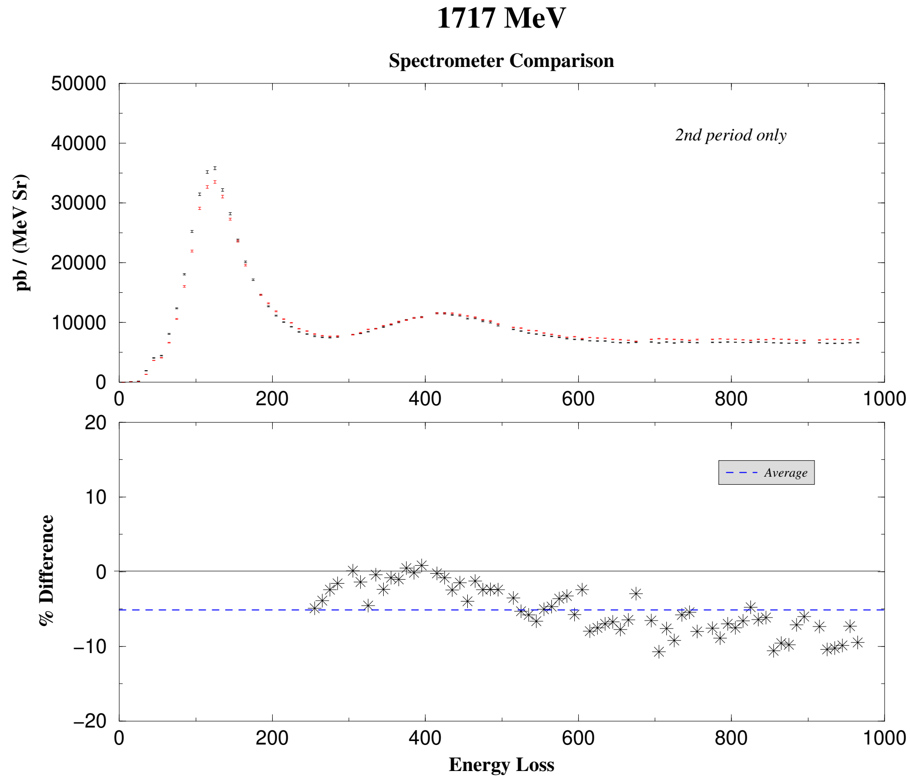

Figure 3: 1717 MeV, 2nd Period. Top Panel: Black electron arm. Red hadron arm. Lower Panel: (E-H)/E X 100. Blue dashed line represents the *unweighted* average.

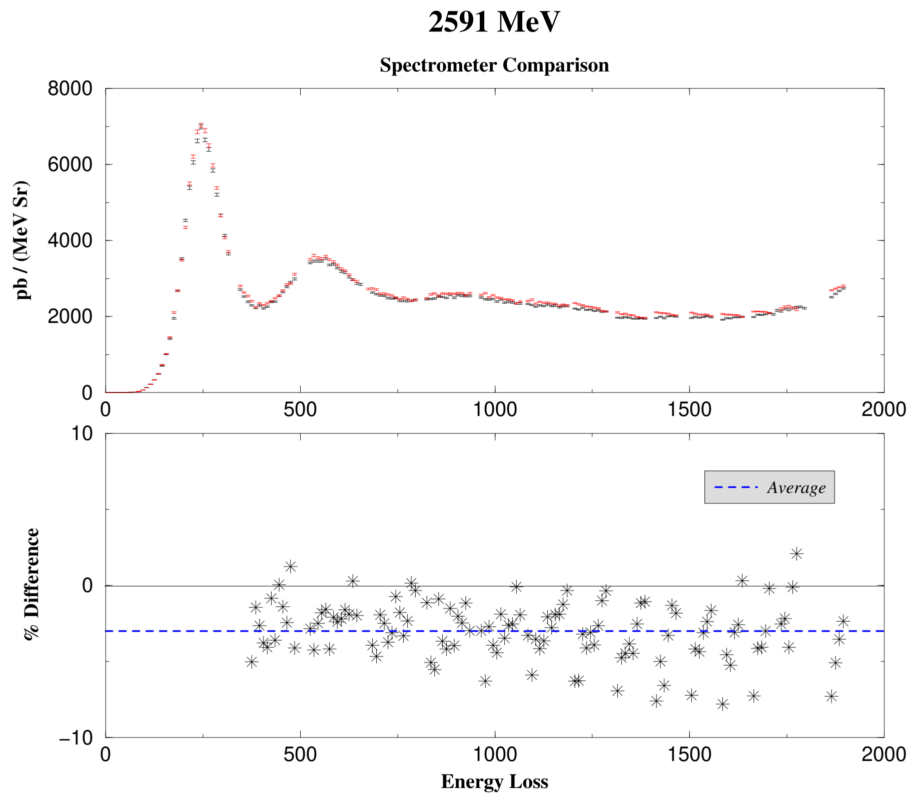

Figure 4: 2591 MeV. Top Panel: Black electron arm. Red hadron arm. Lower Panel: (E-H)/E X 100. Blue dashed line represents the *unweighted* average.

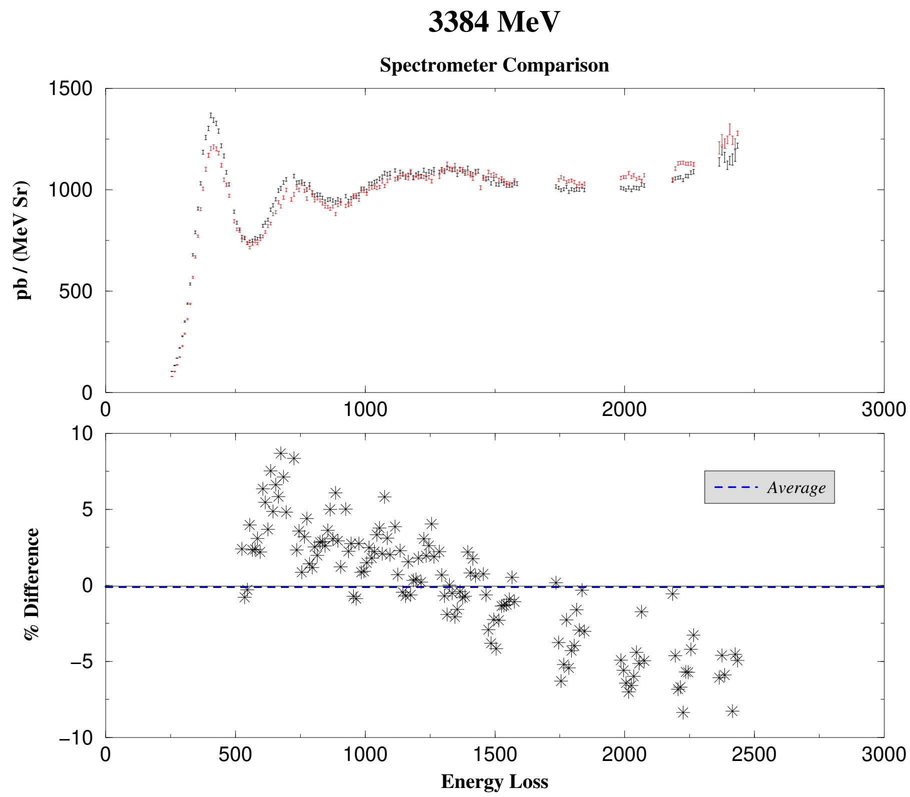

Figure 5: 3381 MeV. Top Panel: Black electron arm. Red hadron arm. Lower Panel: (E-H)/E X 100. Blue dashed line represents the *unweighted* average.

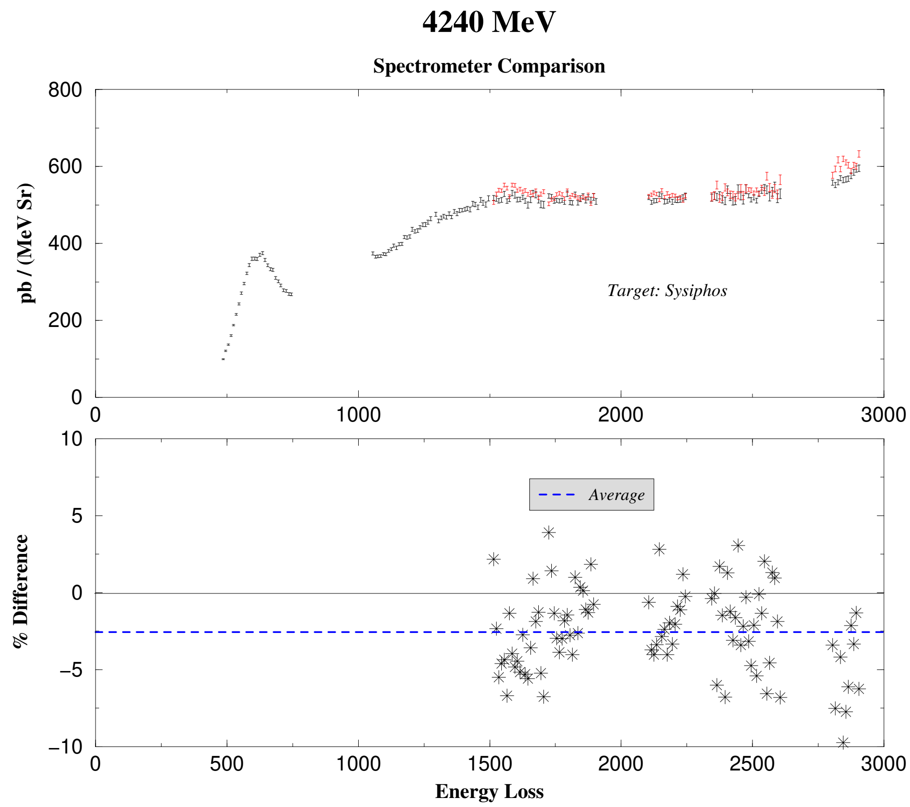

Figure 6: 4239 MeV. Top Panel: Black electron arm. Red hadron arm. Lower Panel: (E-H)/E X 100. Blue dashed line represents the *unweighted* average.

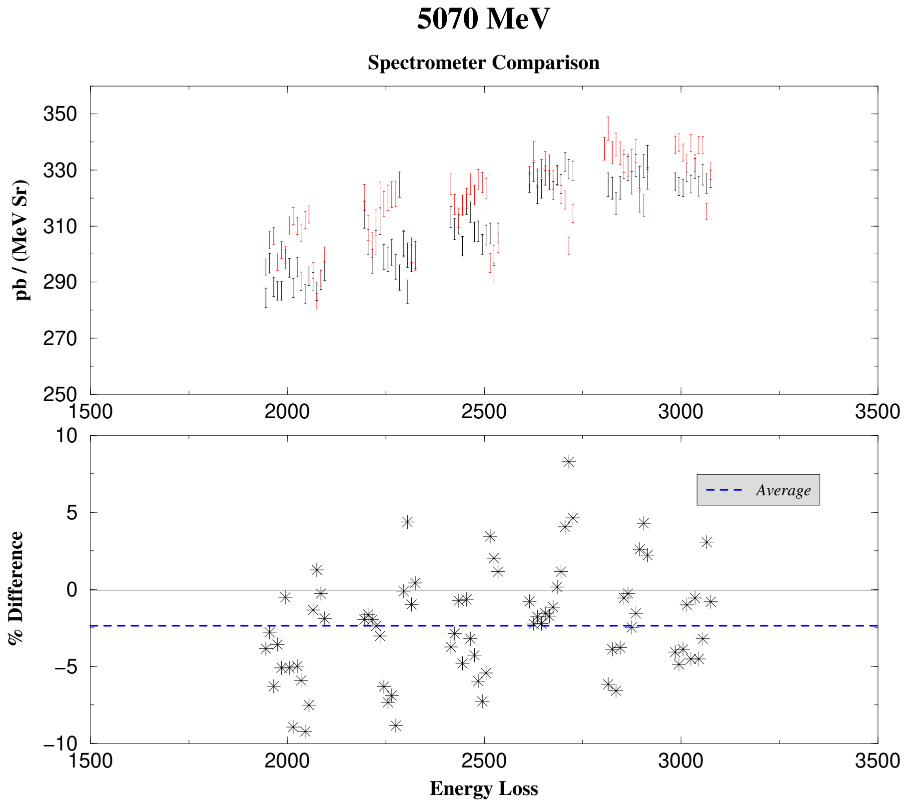

Figure 7: 5058 MeV. Top Panel: Black electron arm. Red hadron arm. Lower Panel: (E-H)/E X 100. Blue dashed line represents the *unweighted* average.

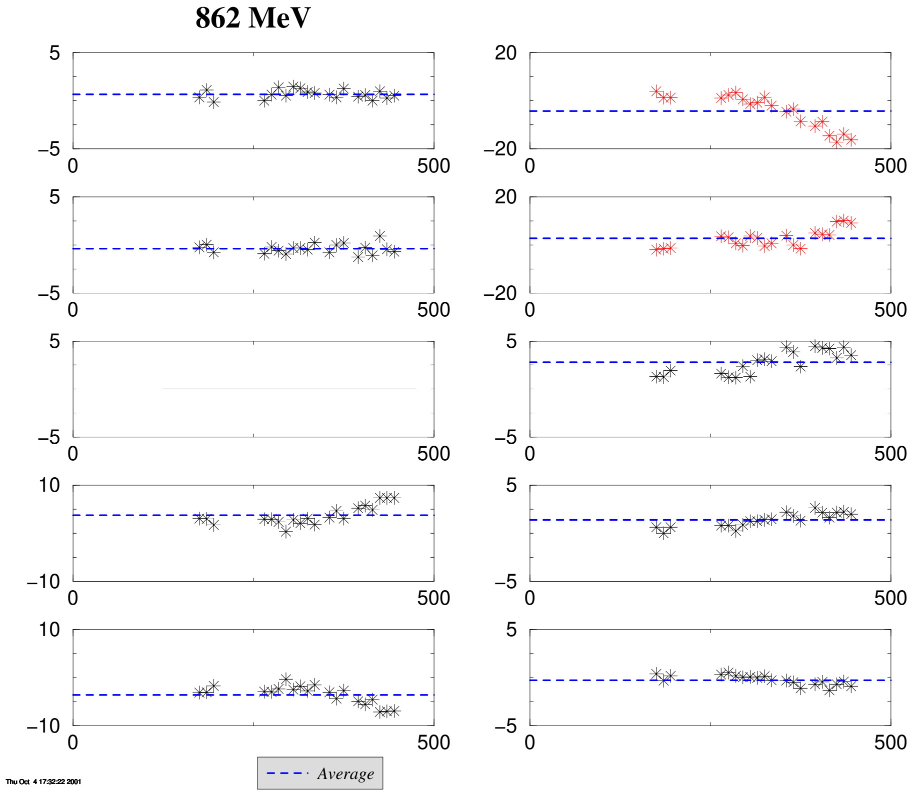

Figure 8: 862 MeV. Comparison of cross section from various cuts of Table 4 to optimized cross section. The percent difference is shown as a function of ν. Column 1 represents cuts 1 to 5. Column 2 represents cuts 6 to 10. Blue dashed line represents the unweighted average.

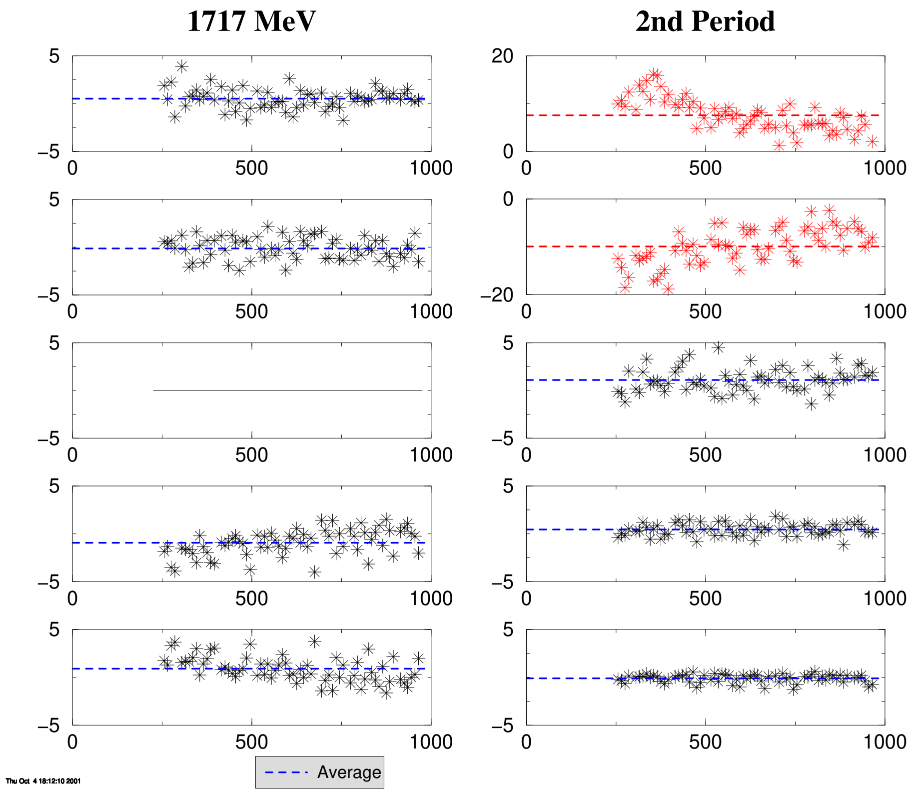

Figure 9: 1717 MeV. Second period.Comparison of cross section from various cuts of Table 4 to optimized cross section. The percent difference is shown as a function of ν. Column 1 represents cuts 1 to 5. Column 2 represents cuts 6 to 10. Blue dashed line represents the unweighted average.

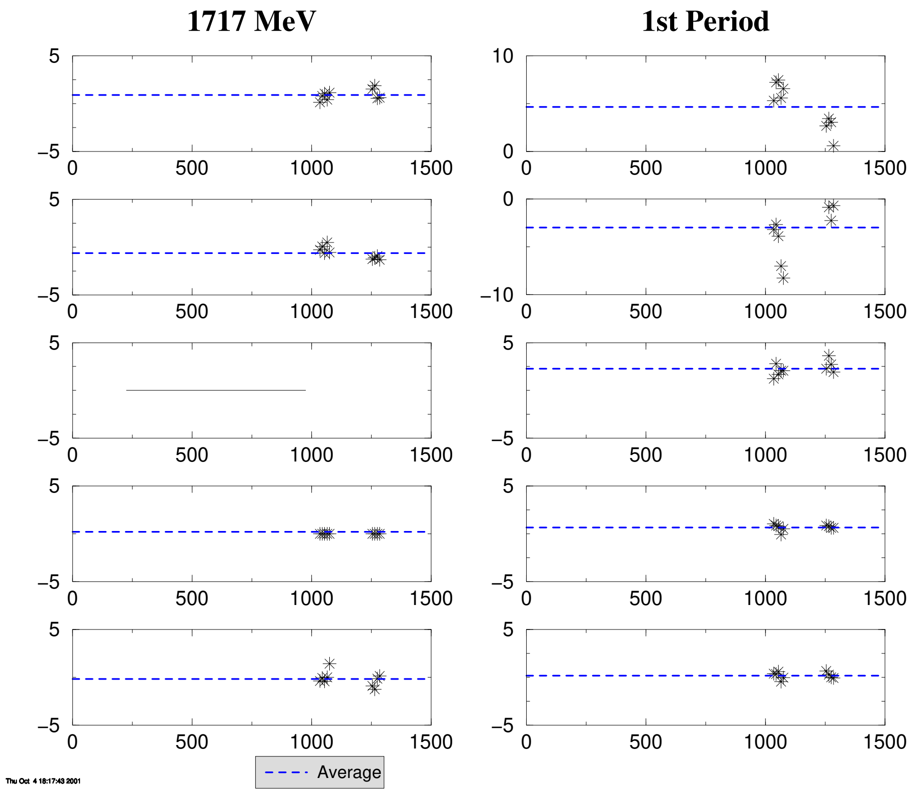

Figure 10: 1717 MeV. 1st period. Comparison of cross section from various cuts of Table 4 to optimized cross section. The percent difference is shown as a function of ν. Column 1 represents cuts 1 to 5. Column 2 represents cuts 6 to 10. Blue dashed line represents the unweighted average.

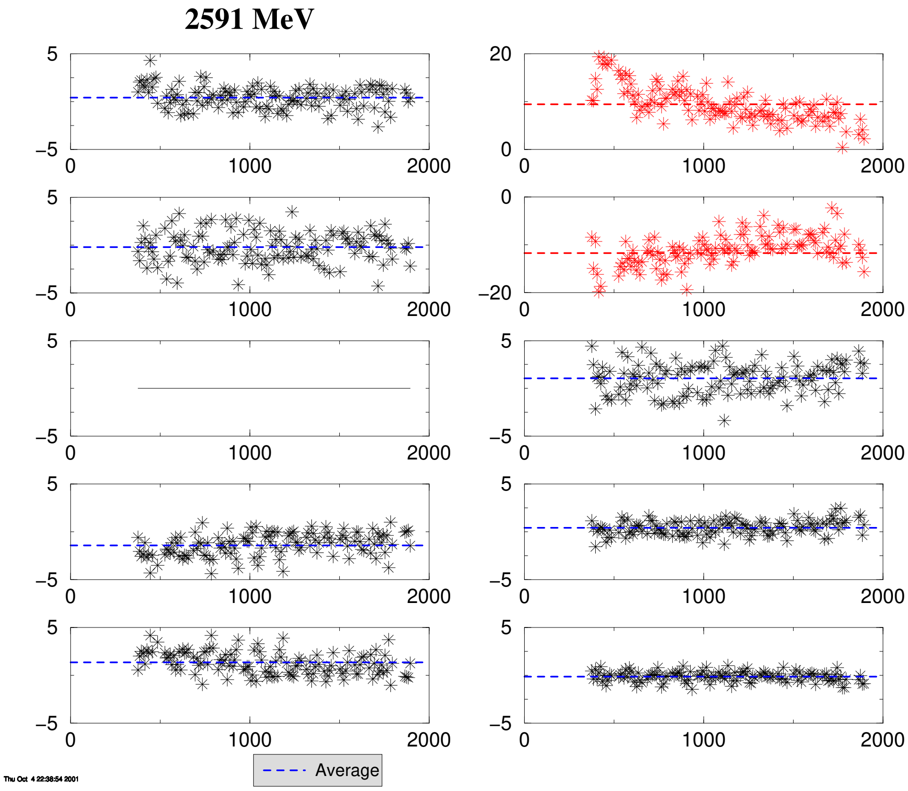

Figure 11: 2591 MeV. Comparison of cross section from various cuts of Table 4 to optimized cross section. The percent difference is shown as a function of ν. Column 1 represents cuts 1 to 5. Column 2 represents cuts 6 to 10. Blue dashed line represents the unweighted average.

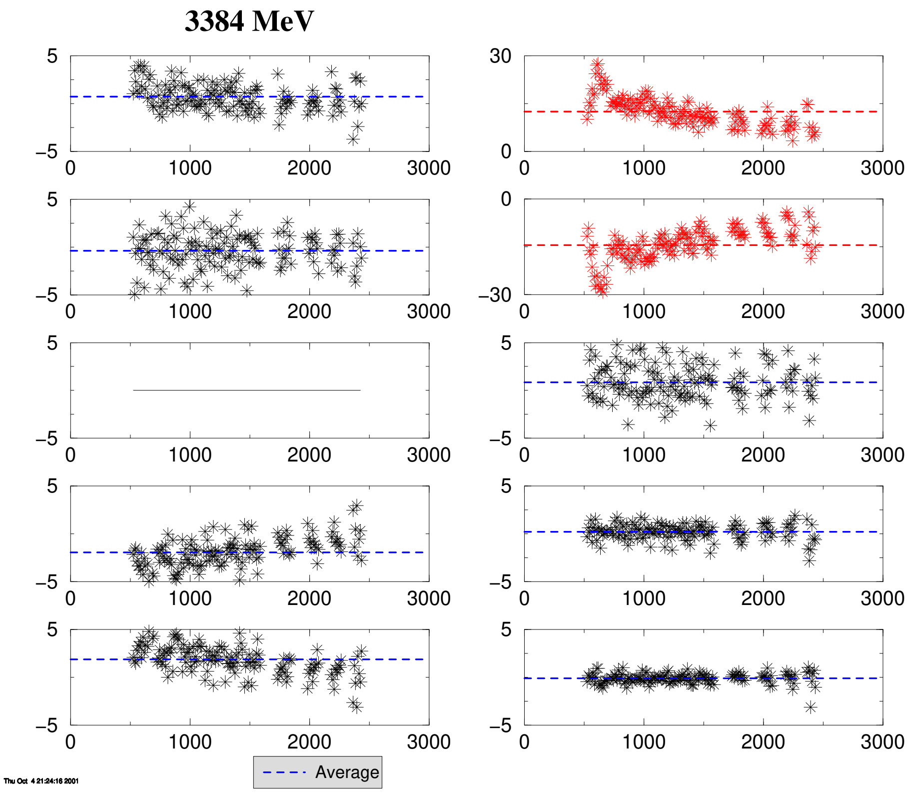

Figure 12: 3382 MeV. Comparison of cross section from various cuts of Table 4 to optimized cross section. The percent difference is shown as a function of ν. Column 1 represents cuts 1 to 5. Column 2 represents cuts 6 to 10. Blue dashed line represents the unweighted average.

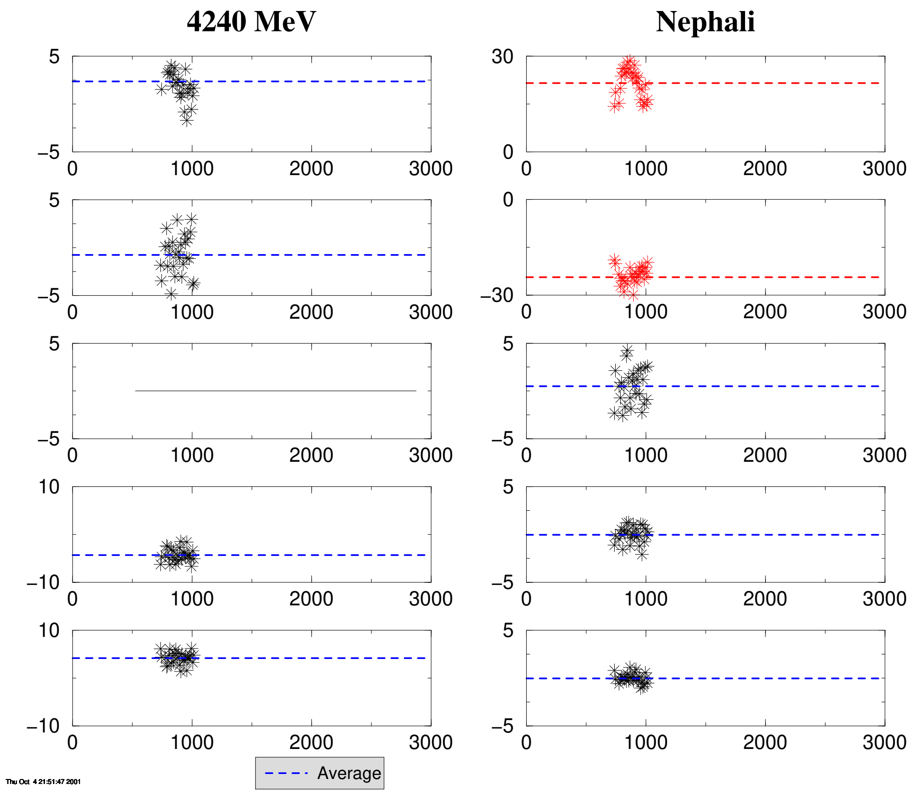

Figure 13: 4239 MeV. Comparison of cross section from various cuts of Table 4 to optimized cross section. The percent difference is shown as a function of ν. Column 1 represents cuts 1 to 5. Column 2 represents cuts 6 to 10. Blue dashed line represents the unweighted average.

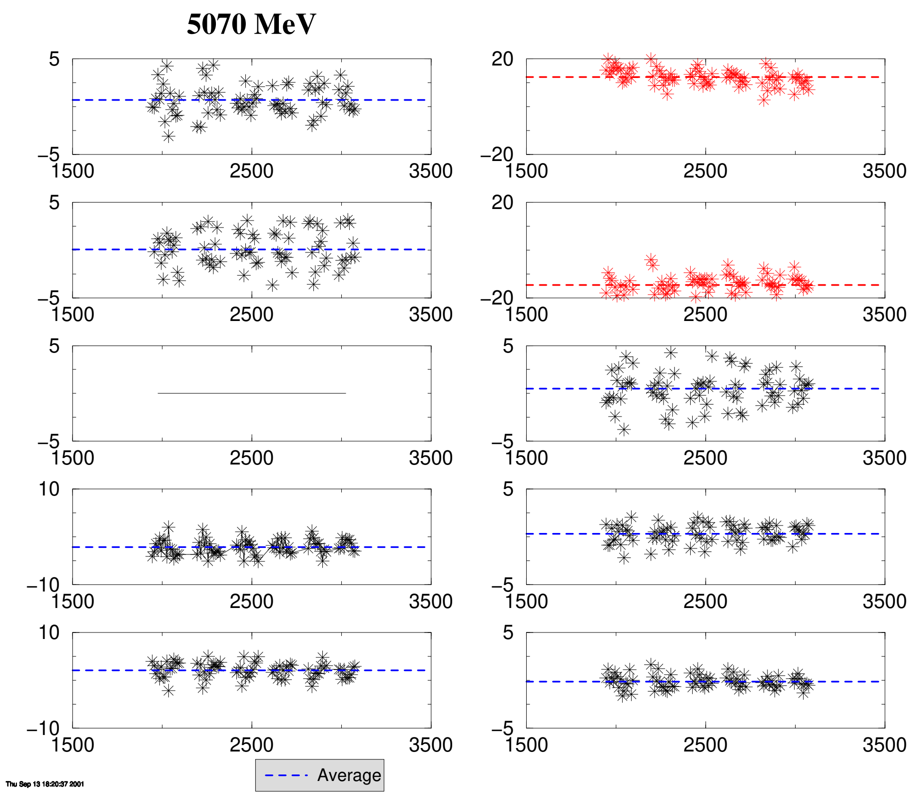

Figure 14: 5058 MeV. Comparison of cross section from various cuts of Table 4 to optimized cross section. The percent difference is shown as a function of ν. Column 1 represents cuts 1 to 5. Column 2 represents cuts 6 to 10. Blue dashed line represents the unweighted average.

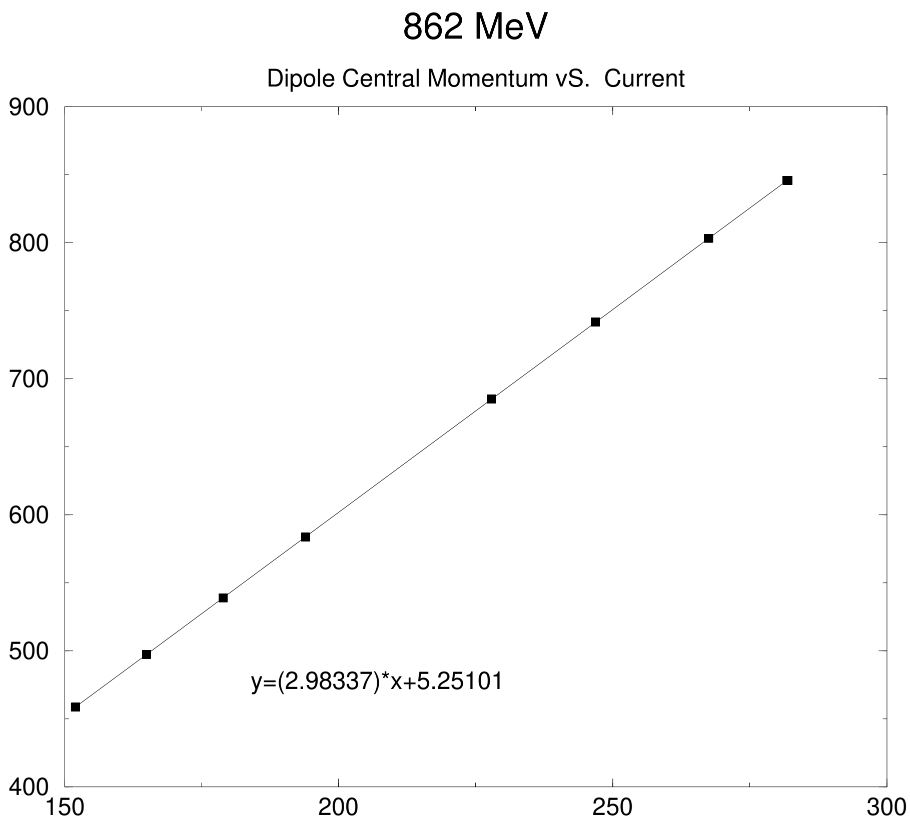

Figure 15: 862 MeV. The central momentum (in MeV) of the electron arm dipole is shown here versus dipole current. The dipole current was used to determine the momentum of the three lowest momentum kinematics (not shown).

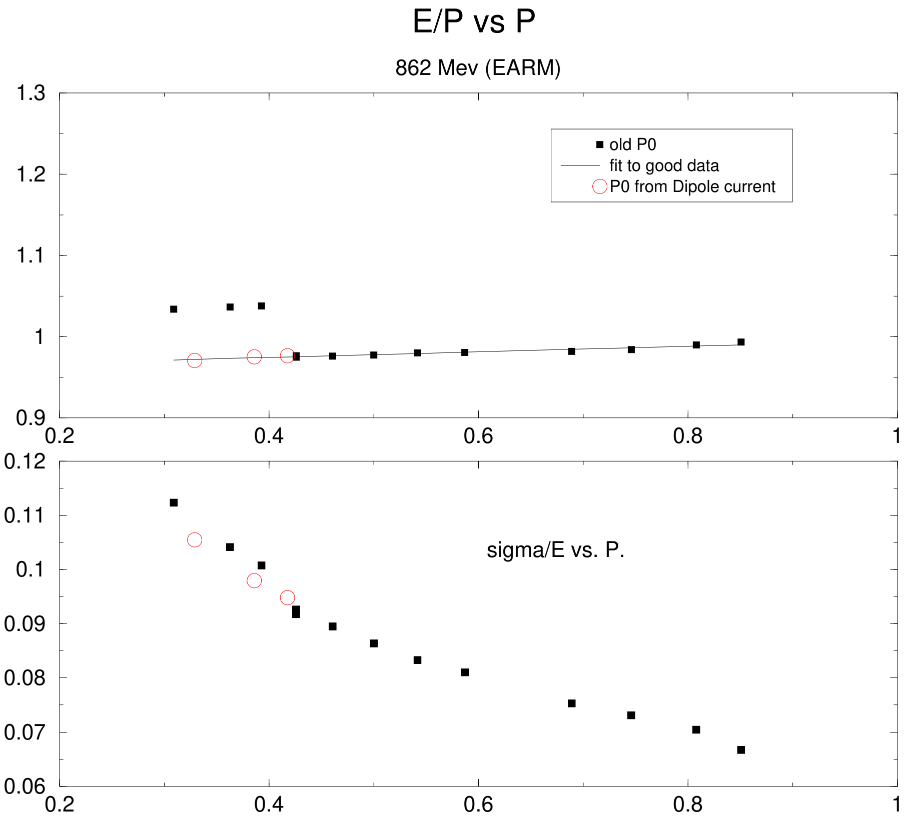

Figure 16: 862 MeV. Top Panel: E/p vs. p. Black squares represent E/p from the calorimeter. Three lowest points indicate miscalibration of the gaussmeter. Solid line is fit to rest of data. Open circles is E/p for lowest three momentum settings when momentum is instead determined from the dipole current. Lower Panel: normalized width σ/E of the E/p spectrum before and after correction.

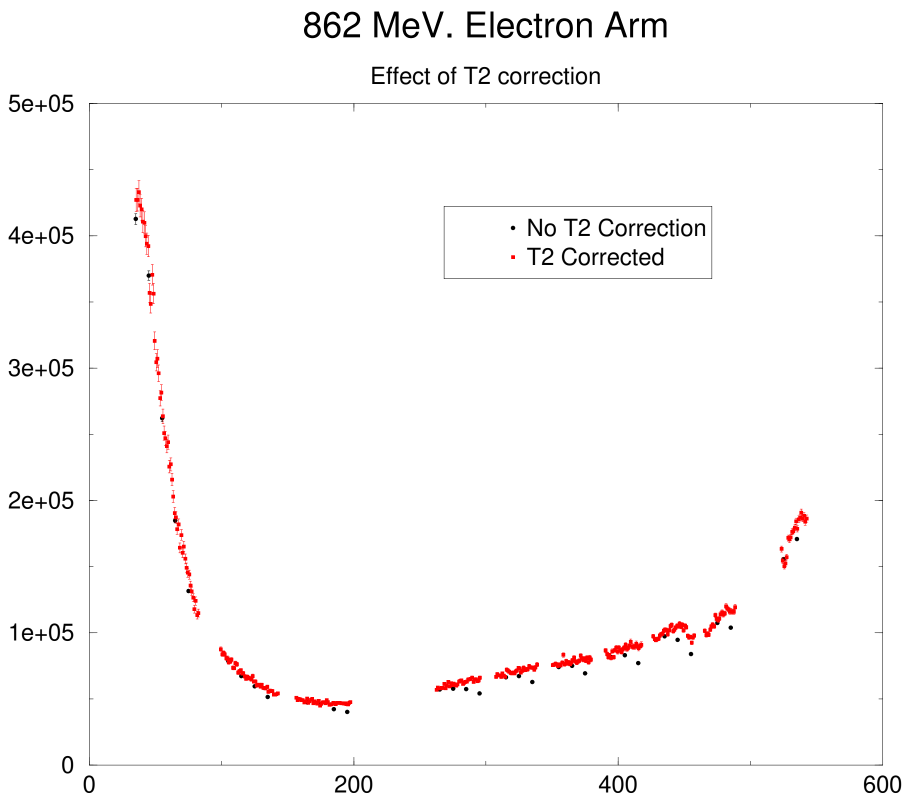

Figure 17: 862 MeV. Black circle: No Scintillator efficiency correction. Red square: With Scintillator correction. Disregard discontinuity at 500 MeV which is caused by quad/dipole mismatch.

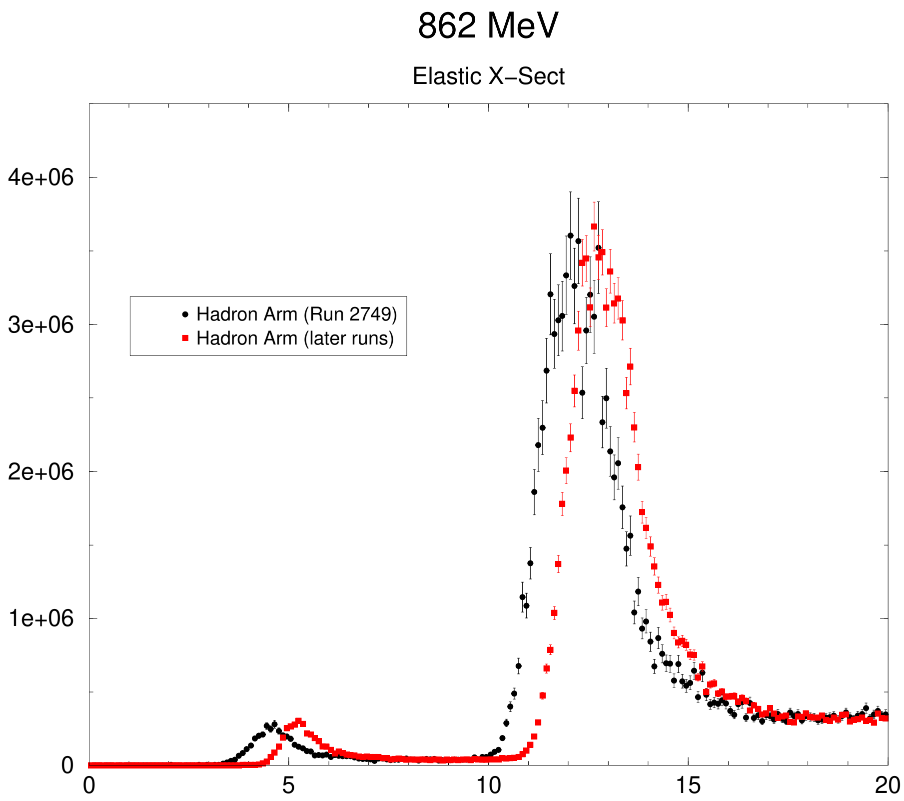

Figure 18: 862 MeV Hadron arm. Shift of elastic peak. Elastic data was taken at the start and at the finish of this energy.

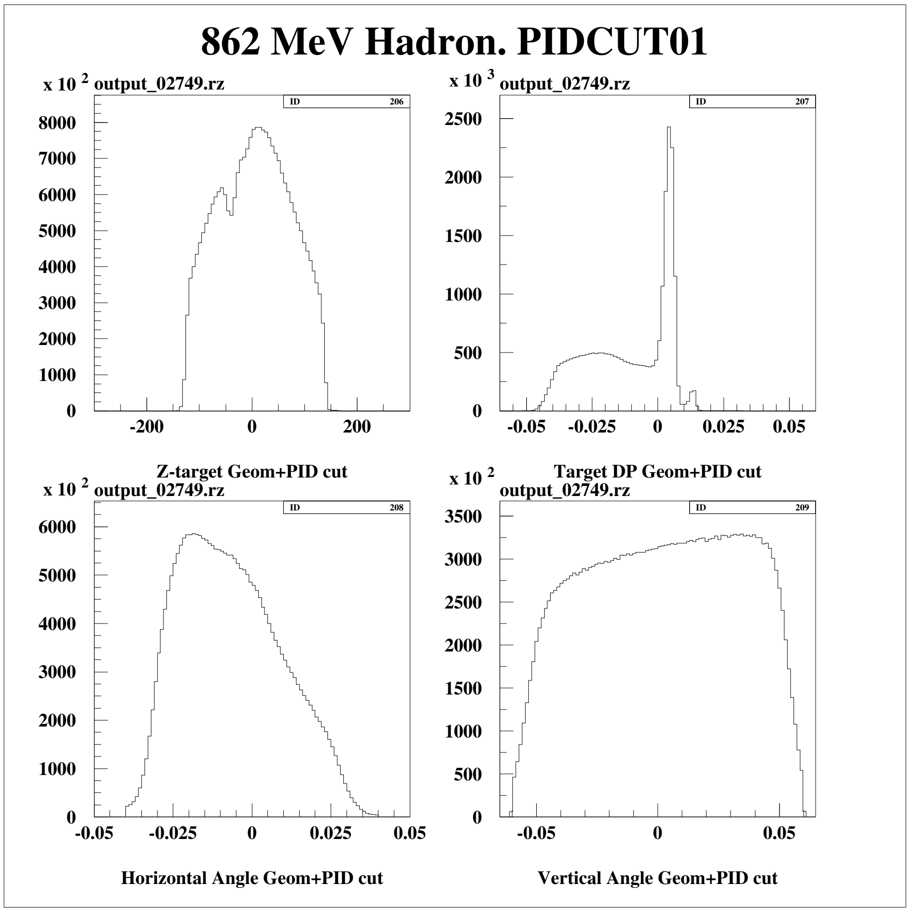

Figure 19: Target Variables for 1st kinematic of 862 MeV.Notice obstruction in negative z-target.

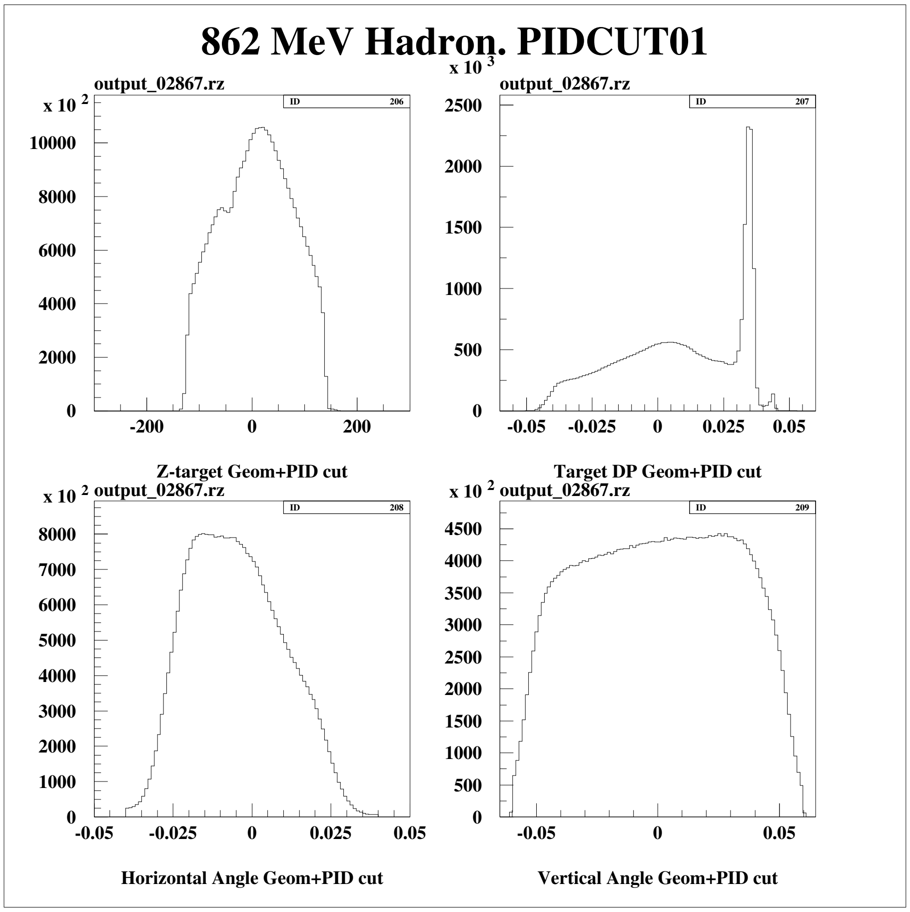

Figure 20: Target Variables for last kinematic of 862 MeV. Notice obstruction in negative z-target.